ACI MATERIALS JOURNAL TECHNICAL PAPER

Title no. 101-M42

Effects of Atmospheric and Construction Conditions on Concrete Equivalent Ages

by Gary S. Wojcik

Concrete maturity, often indicated by its equivalent age, is determined by the interaction of the temperature-dependent exothermic hydration reactions and the atmospheric conditions and curing regimen experienced during early ages. While indexes of concrete maturity have gained wide acceptance in determining proper opening times of structures and in investigations of structural failures, there is a need for a study showing how the maturity in a given structure may change depending on the environmental conditions experienced. In this paper, the SUNY Local Atmosphere Bridge Simulation (SLABS) model is used to predict the equivalent ages of New York State Department of Transportation's Class HP concrete bridge decks for a variety of atmospheric and construction conditions. After 24 h of hydration, the equivalent ages of the same bridge deck vary from 10 h to more than 60 h depending on conditions when averaged over the deck thickness. They also can vary by more than 20 h through the slab thickness. In cases of self-desiccation, the maturity method may provide misleading results.

Keywords: bridge deck; concrete; curing; fly ash; silica fume.

INTRODUCTION

The maturity of concrete is inherently linked to the atmospheric conditions it experiences by the temperature-dependent, exothermic hydration reactions of the concrete's cementitious components. Much research has been done to validate maturity indexes such as the temperature-time factor or the equivalent age (Carino 1984; Carino, Knab, and Clifton 1992; Carino and Tank 1992) that relate the strength of concrete to the temperatures it has experienced for ordinary and high-performance concrete. The importance of understanding the relation between such indexes, concrete strength, and environmental conditions can be seen clearly from investigations of construction failures such as the partial collapses of the Skyline Plaza Apartments in Fairfax County, Va., in March 1973 (Carino et al. 1983) and a cooling tower in Willow Island, W. Va., in 1978 (Lew 1980). For these collapses, which killed 14 and 51 workers, respectively, low air temperature, among other parameters, was cited as a factor in the delayed concrete maturity that contributed to structural failure.

These failure investigations, while beneficial and practical in determining the cause of the failures, are focused on specific conditions and situations. They do not provide insight into how the concrete maturity may have varied if ambient conditions had been different or if the concrete was placed at different times. In this paper, the SUNY Local Atmosphere Bridge Simulation (SLABS) model (Wojcik, Fitzjarrald, and Plawsky 2003) is used to show how concrete maturity (through the equivalent age) varies over a wide range of atmospheric and curing conditions and initial concrete temperatures. Such information will provide engineers and contractors with important information regarding those conditions that may lead to delayed maturity or decreased concrete strength, providing assistance in determining the best time to place concrete or the best curing procedures to obtain the strength needed for safe construction operations. The SLABS model, which predicts the thermal and moisture states of curing concrete, is the first to include all relevant heat transfer processes in its boundary conditions with formulations based on measurements taken at curing concrete bridges. As a result, SLABS can be applied under any atmospheric conditions, with various construction conditions (that is, initial concrete temperature, mixture proportions, and curing regimen).

Maturity method

The maturity method for estimating concrete strength is based on the idea that specimens of the same concrete will acquire equal strength if they acquire equal values of a maturity index. One example of a maturity index is the equivalent age t_e, which is defined as the time it takes for concrete curing at a reference temperature to reach a maturity level equivalent to that obtained for concrete curing at a different temperature (ASTM 1999) and is given by

$$t_e = \sum e^{\left[-\frac{E_a}{R^*}\left(\frac{1}{T_{cavg}}-\frac{1}{T_r}\right)\right]}\Delta t \qquad (1)$$

where

E_a = activation energy (J mol^{-1});
R = ideal gas constant (8.314 J K^{-1} mol^{-1});
Δt = time interval (h or days);
T_{cavg} = average temperature of the concrete during the time interval Δt (K); and
T_r = reference temperature (K).

Equivalent age can be related to strength by using a previously established relationship for the concrete being used. In using Eq. (1) as an indicator of strength development, it is assumed that the initial rate of strength development obeys the Arrhenius equation and that there is sufficient water available for hydration. To implement Eq. (1), it is necessary to know the E_a of concrete, and T_r must be selected. Traditionally, T_r = 293 K (20 °C) has been used (Freiesleben-Hansen and Pedersen 1977), and this value is chosen for this study.

While most maturity indexes are based on concrete temperatures, Kada-Benameur et al. (1999) argue for maturity indexes based on concrete heat fluxes. Their laboratory

ACI Materials Journal, V. 101, No. 5, September-October 2004.
MS No. 03-327 received August 19, 2003, and reviewed under Institute publication policies. Pertinent discussion including authors' closure, if any, will be published in the July-August 2005 *ACI Materials Journal* if the discussion is received by April 1, 2005.

Gary S. Wojcik *is a meteorologist for Northrop Grumman Corporation, Chantilly, Va. He attended the University at Albany, State University of New York (SUNY). His research interests include the effects of environmental conditions on early-age properties, durability of concrete, and the influence of atmospheric conditions on curing concrete bridge temperatures and moisture.*

experiments indicated a change in the sign of the heat flux time derivative when the hydration reactions began generating significant heat. They argue that this is a stronger indicator of the onset of the rapid hydration stage, when rapid strength development begins, than that provided by the concrete temperatures. In a field setting, where heat transfer due to radiation, convection, evaporation, and runoff water heat flux (if water curing is used) (Fig. 1) undergoes typical diurnal cycles, the point at which the heat flux time derivative changes sign during early hydration may be considerably more difficult to interpret. For example, Wojcik and Fitzjarrald (2001) showed from the development of energy balances of four curing concrete bridge decks that the heat flux change at the onset of the rapid hydration stage was similar to that several days later when the concrete was no longer generating significant heat. As was expected, however, during the rapid hydration stage, the total heat transfer through the top surface of curing concrete bridge decks was found to be up to three times higher than that at later ages.

While maturity indexes based on heat fluxes may need further research to be developed and validated, it is precisely the interaction between the heat transfer mechanisms and the hydration reactions that leads to variations in concrete temperatures and maturity. Because the magnitudes and directions of these heat transfer mechanisms can change drastically over the course of a day due to normal atmospheric cycles (Wojcik and Fitzjarrald 2001), all of these mechanisms must be described explicitly for an accurate representation of the total heat transfer and its variation. Only with the proper representation of heat transfer mechanisms can concrete temperatures be accurately predicted. The SLABS model was created with the pertinent atmospheric boundary conditions developed from field measurements at four curing concrete bridges in eastern and central New York State (Wojcik and Fitzjarrald 2001) and a hydration heat mechanism developed with calorimetry experiments (Wojcik, Plawsky, and Fitzjarrald 2001). Peak concrete temperatures and average concrete temperatures over the first 24 h of the active hydration stage were shown to vary by up to 30 °C in the case of bridge decks over a wide range of simulated atmospheric and construction conditions (Wojcik, Fitzjarrald, and Plawsky 2003). Such a wide range of concrete temperatures suggests a wide range of in-place concrete maturity for a bridge deck that has been curing for 24 h.

In the following, the basic components of the SLABS model are discussed, including the governing equations and the boundary conditions. After this, the modeling experiments, which involve varying atmospheric and curing conditions and initial concrete temperatures for SLABS model simulations, are described. Finally, the results of these changes in boundary conditions on concrete temperatures and equivalent ages are discussed.

RESEARCH SIGNIFICANCE

This study provides the first comprehensive view of the effects of a wide range of atmospheric, concrete, and curing conditions on the early-age maturity of concrete as indicated by equivalent ages. The investigation shows that there are many factors that determine early-age concrete temperatures and that all must be accounted for to obtain an accurate prediction of equivalent ages. The information and procedures provided may help engineers and construction personnel determine the best time to place concrete or the best curing practice to use based on atmospheric conditions so that the concrete attains the early-age strength needed to maintain optimal safety during construction.

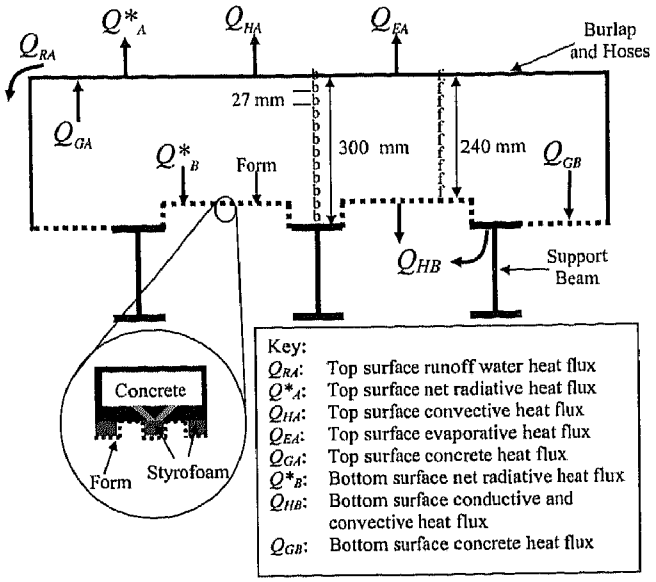

Fig. 1—Schematic cross section of bridge deck indicating energy balance terms used as boundary conditions in SLABS model. Not to scale. Concrete thickness averaged approximately 290 mm for bridges studied and minimum width was 9.8 m. Typical directions of energy flow when peak concrete temperatures occur during night are indicated by arrows. "b" and "f" indicate grid points above beam and form, respectively.

ANALYTICAL INVESTIGATIONS WITH SLABS MODEL

Governing equations

Below is a brief description of the portions of the SLABS model pertinent to the present work. For an expanded view of the model details and performance, refer to Wojcik (2001) and Wojcik, Fitzjarrald, and Plawsky (2003). The SLABS model is a one-dimensional (vertical) finite difference model designed to study heat transfer and generation and moisture movement in curing concrete bridge decks. It solves the governing equations by using a fully implicit Crank-Nicolson scheme for the diffusion of heat and moisture (Press et al. 1989) and a fourth-order Runge-Kutta scheme for the hydration chemistry (Press et al. 1989). Figure 1 shows that the concrete bridge decks that were studied are ≈60 mm thicker over the steel support I-beams (300 mm deep) than they are over the form (240 mm deep), a corrugated, galvanized steel sheet. The finite difference model consists of 10 vertical grid points (nine layers) above the form and 12 vertical grid points (11 layers) above the beams, with a grid size of 27 mm. For the bridges studied, moist curing of the decks with burlap and spray water from irrigation hoses was used.

The concrete simulated for this study is a New York State Department of Transportation (NYSDOT) Class HP mixture,

the cementitious component of which consists of 74% ASTM Type I, Type II, or Type I/II cement, 20% Class F fly ash, and 6% silica fume by mass (NYSDOT 1999). Class HP concrete has a water-cementitious material mass ratio (*w/cm*) of 0.38. The hydration reactions are modeled as a bimolecular reaction between the cementitious material and the water (Wojcik, Plawsky, and Fitzjarrald 2001). The change in the unhydrated cementitious materials concentration B is given by

$$\frac{dB}{dt} = -k \cdot B^n \cdot R^m \tag{2}$$

where

B = concentration of unhydrated cementitious materials (mol m^{-3});
R = concentration of water available for hydration reactions (mol m^{-3});
n, m = exponents, the sum of which gives the order of hydration reactions;
k = reaction rate constant (m^3 mol^{-1} s^{-1}); and
t = time, s.

The reaction rate constant k is given by

$$k = A \cdot \exp\left(-\frac{E_a}{R^* \cdot T_c}\right) \tag{3}$$

where

A = pre-exponential factor; and
T_c = concrete temperature (K).

Wojcik, Plawsky, and Fitzjarrald (2001) determined that $n = m = 1$ and $E_a = 35$ kJ mol^{-1} for Class HP cementitious material through the method of excess (Fogler 1992) and constant temperature calorimetry. In applying these methods, the cementitious material hydrated in water that had a concentration large enough that it essentially did not vary in time during hydration. Note that this value of E_a is used also in Eq. (1). Wojcik, Fitzjarrald, and Plawsky (2003) determined that $A = 0.0039$. The governing equation for concrete temperature T_c is given by

$$\frac{dT_c}{dt} = K_T \frac{\partial^2 T_c}{\partial z^2} - V \cdot \frac{dB}{dt} \tag{4}$$

where

V = a parameter that converts reacted cementitious material concentration to evolved heat and is equal to $-\Delta H M_{wB}/\rho_c c_{pc}$ (K m^3 mol^{-1} s);
c_{pc} = specific heat capacity of Class HP concrete (1380 J kg^{-1} K^{-1});
$-\Delta H$ = Class HP concrete heat of hydration (≈420 kJ kg^{-1}; Wojcik, Plawsky, and Fitzjarrald 2001);
z = vertical dimension, m;
k_c = Class HP concrete thermal conductivity (≈2.7 W m^{-1} K^{-1});
ρ_c = density of Class HP concrete (2230 kg m^{-3});
K_T = thermal diffusivity of concrete (≈8.8×10^{-7} m^2 s^{-1}), obtained from the values of ρ_c, c_{pc}, and k_c [$K_T = k_c/(c_{pc}\rho_c)$] (Wojcik and Fitzjarrald 2001; Wojcik, Plawsky, and Fitzjarrald 2001); and
M_{wB} = molecular mass of the cementitious material (≈0.2 kg mol^{-1}) determined from a mass average weighting of molecular weights of cement, fly ash, and silica fume.

The second term on the right-hand side of Eq. (4) is the hydration heat source term.

The available water concentration R (mol m^{-3}) is given by

$$\frac{dR}{dt} = K_R \frac{\partial^2 R}{\partial z^2} + \eta \cdot \frac{dB}{dt} \tag{5}$$

where

K_R = diffusivity of water in concrete (≈10^{-9} m^2 s^{-1}; Pommersheim and Clifton [1991]);
R = water concentration in the concrete that is available for hydration reactions; and
η = number of moles of water removed from the available water per mole of cementitious material that hydrates.

The water diffusivity K_R is reduced by a factor of 20 (Powers 1958) when the hydration fraction reaches 0.6. At this hydration fraction in conjunction with the *w/cm* of Class HP concrete, the larger pores in the paste become depercolated (Bentz and Garboczi 1991; Garboczi and Bentz 2001), significantly limiting the movement of water. The term η includes water that is chemically converted into hydration products and water that is adsorbed onto the surface of the hydration products where it cannot be used for further hydration (Powers and Brownyard 1946a,b,c, 1947a,b,c,d). Wojcik, Fitzjarrald, and Plawsky (2003) determined that $\eta = 8.3$.

Boundary conditions

At the top and bottom surfaces of the bridge deck, the boundary conditions are implemented in flux conservative form (for example, Press et al. 1989) to maintain the stability of the solutions by keeping the second order accuracy of the Crank-Nicolson diffusion scheme. By convention, upward fluxes are positive.

At the top surface, the energy balance (Wm^{-2}) is given by

$$-Q_A^* + Q_{GA} = Q_{EA} + Q_{HA} + Q_{RA} \tag{6}$$

where

$-Q_A^*$ = net radiation (net shortwave + net longwave);
Q_{GA} = heat flux through top surface of concrete;
Q_{HA} = convective sensible (that which can be felt) heat flux;
Q_{EA} = evaporation heat flux; and
Q_{RA} = runoff water heat flux (Fig. 1).

The total top surface energy flux is given by

$$Q_{GA} = -k_c \frac{dT_c}{dz} = \tag{7}$$

$$Q_A^* - \rho L_v C_e U(q_a - q_s) - \rho c_p C_h U(T_a - T_s)$$

$$-\rho_w c_w (T_{wi} - T_{wf}) \frac{SW}{A_{top}}$$

where

SW = volume flow rate of spray water running off the bridge (m^3 s^{-1});

A_{top} = area of bridge deck's top surface (m^2);
q_a and q_s = ambient air and near-surface specific humidities (g g^{-1});
T_a and T_s = air and surface temperatures, °C;
ρ_w and ρ = water and air densities (kg m^{-3});
c_w and c_p = water and air specific heat capacities (J kg^{-1} K^{-1});
C_e and C_h = dimensionless exchange coefficients;
T_{wi} and T_{wf} = initial (when hitting top surface) and final (when running off bridge) spray water temperatures, °C;
L_v = latent heat of evaporation (J kg^{-1}); and
U = wind speed (m s^{-1}).

The second term on the right-hand side of Eq. (7) is the evaporative heat flux, the third is the sensible heat flux, and the fourth is the runoff water heat flux. See Wojcik, Fitzjarrald, and Plawsky (2003) and Wojcik and Fitzjarrald (2001) for more information on the exchange coefficients.

The net radiation Q_A^*, the dominant term in the top surface energy balance (Wojcik and Fitzjarrald 2001), is computed by determining the incoming and outgoing longwave and shortwave radiation components. The clear sky, incoming shortwave radiation at the surface is calculated with a scheme given by Stull (1988). The effect of cloud cover fraction on the incoming shortwave radiation is given by Freedman et al. (2001) as

$$K_I = [0.91 - (0.7 \cdot clf)] \cdot K_{clear} \quad (8)$$

where
K_I = incoming shortwave radiation at surface (W m^{-2});
K_{clear} = clear sky, incoming shortwave radiation at surface (W m^{-2}); and
clf = cloud cover fraction.

The albedo (fraction of incoming solar radiation that is reflected by a surface) of concrete covered with burlap and sprayed with water was determined to be 0.14 (Wojcik and Fitzjarrald 2001). Therefore, the outgoing shortwave radiation K_O is equal to $0.14 \cdot K_I$.

For clear skies, the incoming longwave radiation is given by Stefan-Boltzman's law. The clear skies atmospheric emissivity, as a function of atmospheric water vapor pressure and air temperature, is determined with a scheme proposed by Prata (1996)

$$\varepsilon_{clear} = 1 - \left(1 + 4.65 \cdot \frac{e_a}{T_a}\right) \cdot \exp\left\{-\left(1.2 + 3 \cdot 46.5 \cdot \frac{e_a}{T_a}\right)^{\frac{1}{2}}\right\} \quad (9)$$

where
ε_{clear} = clear skies atmospheric emissivity; and
e_a = atmospheric water vapor pressure (millibars).

The cloudy skies atmospheric emissivity, as a function of vapor pressure, temperature, and clf, is given by Brutsaert (1975)

$$\varepsilon_{cloudy} = clf + 1.24 \cdot (1 - clf) \cdot \left(\frac{e_a}{T_a}\right)^{\frac{1}{7}} \quad (10)$$

where ε_{cloudy} = cloudy skies atmospheric emissivity.

Stefan-Boltzman's law is also used to compute the outgoing longwave radiation with a surface emissivity of 0.98 for the wet surfaces of the bridges.

The spray water drops will adjust to the environmental conditions as they rise and fall after being ejected from the irrigation hoses. Because the drops do not remain airborne for more than a few seconds, their temperatures generally do not approach the air wet-bulb temperature. Therefore, a model by Pruppacher and Klett (1997) is used to calculate the temperature of the spray water as it hits the top surface (T_{wi}). The runoff water temperature (T_{wf}) is assumed to equal the top surface concrete temperature, as suggested by Wojcik and Fitzjarrald (2001). For the top surface water boundary condition when the effects of spray water are considered, it is assumed that there is a puddle of water on the top surface, giving a water concentration R of 55,555 mol m^{-3}.

Heat transfer at the sheet metal form is generally small and is dominated by Q_B^*. The net radiation at the form is generally $-25 \text{ W m}^{-2} < Q_B^* < 25 \text{ W m}^{-2}$ much of the time (Wojcik and Fitzjarrald 2001). To model the heat transfer through the top of the steel support beams (Fig. 1), a formulation of heat flow through an infinite steel fin (Incropera and DeWitt 1996) is used. This localized beam heat transfer can be up to 150 W m^{-2} during the active stage of the hydration reactions, or approximately 50% of that at the top surface during this time (Wojcik and Fitzjarrald 2001). The resulting horizontal temperature gradients near the bottom of the deck may be as large as the vertical gradients at the top surface (Wojcik, Fitzjarrald, and Plawsky 2003). Refer to Wojcik, Fitzjarrald, and Plawsky (2003) for complete details of the bottom surface heat transfer.

The SLABS model was found to predict concrete temperatures over the entire slab to within 2 °C of the observed temperatures both during the time of peak concrete temperatures and when the concrete is no longer generating significant heat and is more passive in its environment (Wojcik, Fitzjarrald, and Plawsky 2003). Predicted energy balances at the top surfaces of the bridge decks were within 30% of those determined from field observations. The model was validated with data from four field measurement campaigns at curing concrete bridges, the most extensive bridge campaigns to date. The model can only be improved and its performance evaluated more fully when more field data have been collected.

Boundary condition sensitivity studies

The equivalent ages of concrete in the bridge deck were calculated for a variety of atmospheric and construction conditions for the first 24 h after placement. The atmospheric variables considered were air temperature T_a and relative humidity RH, wind speed U, and cloud cover fraction clf, which affects radiation. The ranges of values chosen represent typical atmospheric conditions (Table 1). The construction variables that were considered include the spray water flow rate over the deck (SW), the initial temperature of the spray water as it left the hoses (T_{a0}), the concrete temperature at the time of placement (T_{c0}) (Table 1), and the local time of

Table 1—Baseline values and ranges of values*

		Baseline	Range
Atmospheric variables	T_a, °C	25	0 to 45†
	RH, %	70	0 to 100‡
	U, m s^{-1}	3	0.5 to 10§
	clf	0	0 to 1
Construction variables	SW, m^3 h^{-1}	4	0 to 14
	T_{c0}, °C	25	5 to 40
	T_{d0}, °C	25	5 to 40

*Of atmospheric and construction values used in SLABS model simulations.
†Afternoon-morning temperature pairs, °C: 45-35, 40-30, 35-25, 30-20, 25-15, 20-10, 15-5, and 10-0.
‡Afternoon-morning relative humidity pairs, %: 0-0, 0-60, 10-70, 20-80, 30-90, 40-100, 100-100.
§Afternoon-morning wind speed pairs, m s^{-1}: 10-0.5, 8-0.5, 6-0.5, 4-0.5, 2-0.5, 0.5-0.5.

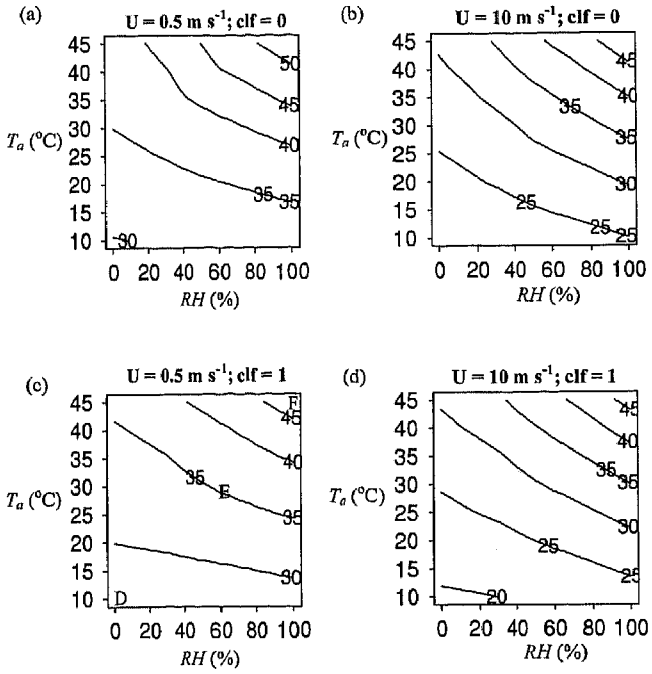

Fig. 2—Predicted concrete temperatures averaged over 10 vertical model grids over period of time used to compute equivalent ages, as a function of afternoon RH and afternoon air temperature T_a *with afternoon wind speed* U *and cloud cover fraction* clf *set as indicated above each figure. All other variables are set to baseline values as shown in Table 1.*

placement *LTP*. These construction variables can potentially be controlled by the construction personnel or the field engineer. For the bridges that were studied in the field, *SW* ranged from 0.6 to 4 m^3 h^{-1}. The values of T_{c0} ranged from 23 to 29 °C, and the values of T_{d0} ranged from 15 to 29 °C. The ranges of these variables were expanded for the construction practice simulations to broaden the scope of the investigation.

Diurnal variations of the atmospheric variables were approximated with simple cosine functions that capture the main features of typical diurnal variations (Wojcik, Fitzjarrald, and Plawsky 2003). The air temperature T_a and wind speed U generally peak during the late afternoon, while *RH* reaches a minimum during this time. The variations of incoming solar radiation with time of day and time of year were

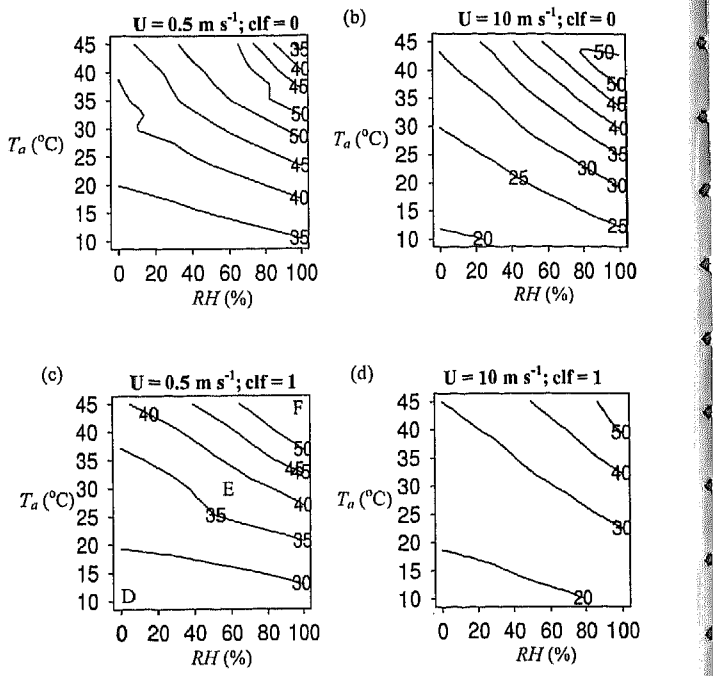

Fig. 3—Predicted equivalent ages after 24 h of hydration averaged over the 10 vertical model grids as a function of afternoon RH and afternoon air temperature T_a *with afternoon wind speed* U *and cloud cover fraction* clf *set as indicated above each figure. All other variables are set to baseline values as shown in Table 1.*

computed with schemes from Stull (1988). The simulations were run for Albany, N.Y. in early June with the concrete being placed at 0700 local time (LT).

The length of the dormant period or induction period was set at 8 h, as was observed at the bridges studied in the field and from laboratory calorimetry experiments on cementitious components and admixtures from the stocks used for the bridges (Wojcik and Fitzjarrald 2001; Wojcik, Plawsky, and Fitzjarrald 2001; Wojcik, Fitzjarrald, and Plawsky 2003). The influence of set-retarding admixtures on the length of the dormant period often can be a function of the temperature at which they are used (Neville 1996). Specific information about the influence of temperature is not available for those admixtures used in the bridges upon which the SLABS model is based, however. Therefore, the effect of temperature on the retarders is not considered in the model at this time.

The equivalent ages were computed using Eq. (1), and the concrete was allowed to mature as long as there was water available for reaction at a given grid point. When the available water was used up at a given location, the values of t_e no longer accumulated. Because the form bounds approximately 80% of the deck concrete from below, only simulations over the form were considered.

RESULTS

Equivalent age sensitivity to atmospheric conditions

When averaged over the 10 vertical grid points of the simulated Class HP slab, concrete temperatures (Fig. 2) and equivalent ages t_e (Fig. 3) are generally maximum when high air temperatures and humidities influenced the curing concrete. Under these conditions, evaporation and convection are limited, allowing the concrete to retain heat. The equivalent

ages averaged throughout the depth at 24 h varied between 18 and 55 h (Fig. 3).

Note that in Fig. 3(a) the values of t_e are reduced at the highest air temperatures and humidities. The reason for this is that for these simulations, with light wind speeds, the convective and evaporative heat fluxes are low, which allows the concrete temperatures to reach their maximum (reaching a peak of 64 °C [data not shown]) near the bottom of the concrete slab. With such high temperatures, hydration is extremely rapid, quickly using up the available water. Because curing water from the top surface does not penetrate below the top two or three grids (Wojcik, Fitzjarrald, and Plawsky 2003), this water is not replenished. With no available water, the concrete cannot continue to mature and lower equivalent ages result. While this self-desiccation has not been verified directly for Class HP concrete, it is possible given that Class HP concrete contains 26% cement replacement with fly ash and silica fume by mass (for example, Hooton 1993) and that *w/cm* = 0.38. Note that if it were assumed that there was sufficient water under these conditions, the value of t_e would continue to increase smoothly as T_a and RH increase and would reach a peak of 70 h.

The actual strength of the concrete at 24 h under high T_a and RH conditions is likely to be slightly higher than that under more moderate conditions (for example, afternoon T_a = 30 °C and RH = 60%) because the cementitious material hydration fractions are higher under the extreme conditions (0.49 versus 0.48; data not shown). The equivalent ages, however, suggest that the concrete cured under high T_a and RH conditions (Fig. 3(a)) would have a lower strength at 24 h than that under more moderate conditions. This analysis, then, shows that the maturity method can be misleading or unreliable when applied to concrete in which self-desiccation occurs.

Increasing the wind speed and the cloud cover fraction lowers the equivalent ages, with the wind speed having the larger effect of these two variables. For example, increasing the wind speed from 0.5 to 10 m s^{-1} lowers the equivalent age from 32 to 19 h for T_a = 10 °C, RH = 0%, and *clf* = 0 (Fig. 3(a) and (b)). When the cloud cover fraction is increased from *clf* = 0 to *clf* = 1, t_e is lowered from 32 to 26 h at T_a = 10 °C, RH = 0%, and U = 0.5 m s^{-1} (Fig. 3(a) and (c)). Higher wind speeds allow more efficient convective and evaporative heat loss, lowering concrete temperatures and thus the equivalent ages. Increasing the cloud cover fraction reduces incoming solar radiation, producing lower concrete temperatures and equivalent ages.

Equivalent age sensitivity to construction conditions

Variations in the initial concrete temperatures T_{c0}, spray water flow rate *SW*, and the initial spray water temperatures T_{d0} produce average concrete temperatures that range from 18 to 41°C (Fig. 4) and values of t_e that range from 16 to 50 h (Fig. 5). The highest equivalent ages occur when the initial concrete temperatures and spray water temperatures are high and when the spray water flow rate is low. The concrete maturity is most sensitive to the initial concrete temperatures when the spray water flow rate is low. For example, the equivalent age increases from 25 to 50 h over the T_{c0} range when *SW* approaches 0 m^3 h^{-1} and wind speed U = 0.5 m s^{-1} (Fig. 5(a)). When *SW* = 14 m^3 h^{-1}, however, t_e increases from 16 to 25 h over the range of T_{c0}. At lower *SW*, the runoff water heat flux is not as effective in modulating concrete temperatures as when *SW* is high.

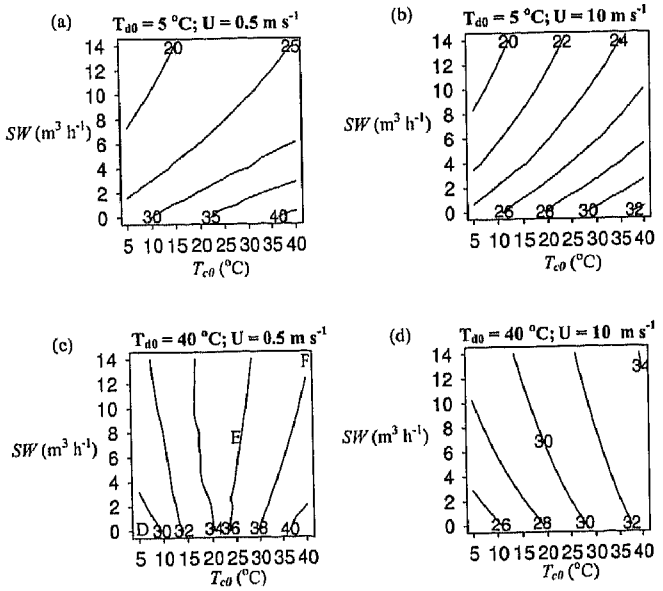

Fig. 4—Predicted concrete temperatures averaged over ten vertical model grids over the period used to compute equivalent ages as a function of spray water volume SW *and initial concrete temperature* T_{c0} *with initial spray water temperature* T_{d0} *and afternoon wind speed* U *set to values indicated above each figure. All other variables are set at baseline values given in Table 1.*

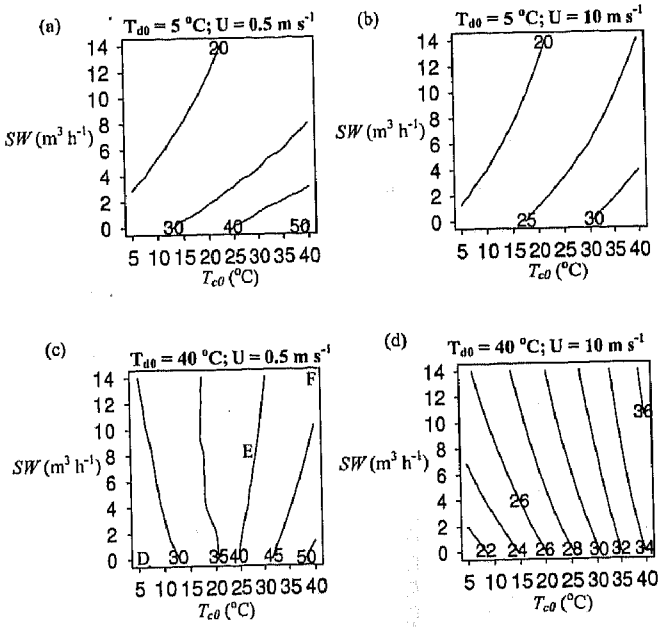

Fig. 5—Predicted equivalent ages after 24 h of hydration averaged over 10 vertical model grids as a function of spray water volume SW *and initial concrete temperature* T_{c0} *with initial spray water temperature* T_{d0} *and afternoon wind speed* U *set to values indicated above each figure. All other variables are set at baseline values given in Table 1.*

In general, greater values of t_e result when concrete is placed in the early morning, which results in higher concrete temperatures (data not shown). Such a placement time results in higher concrete temperatures because the concrete is exposed to solar radiation during the dormant period, allowing it to warm. Concrete placed in the late afternoon

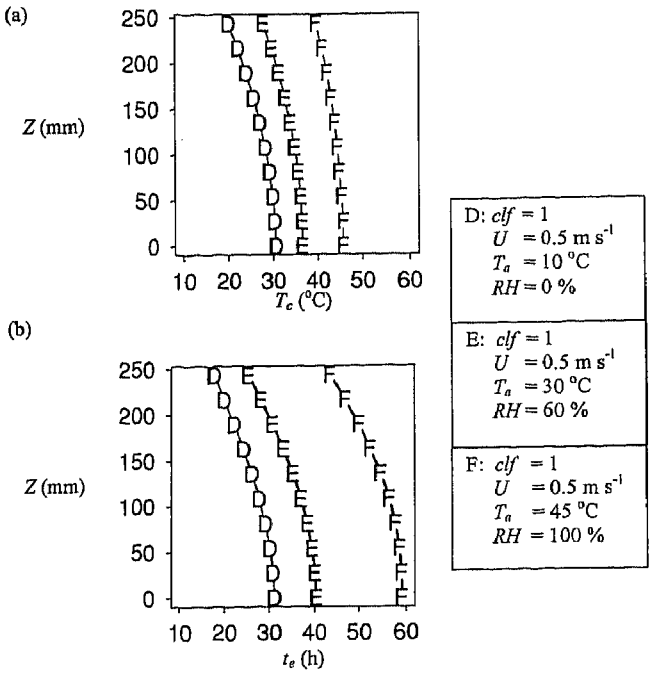

Fig. 6—(a) Vertical concrete temperature profiles; and (b) vertical equivalent age profiles for scenarios indicated in Fig. 2(c) and 3(c), respectively, by D, E, and F. Z (mm) indicates distance from above the form.

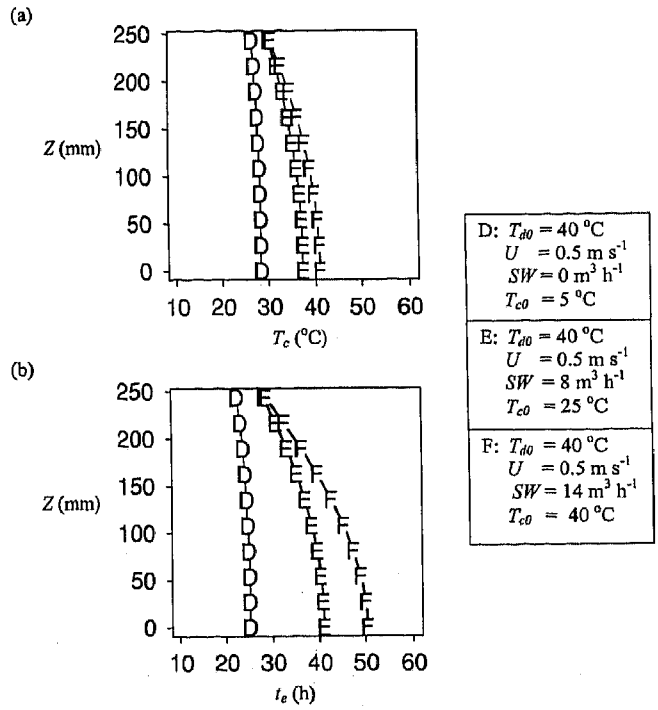

Fig. 7—(a) Vertical concrete temperature profiles; and (b) vertical equivalent age profiles for scenarios indicated in Fig. 4(c) and 5(c), respectively, by D, E, and F. Z (mm) indicates distance from above the form.

cools during the dormant period. Therefore, when the rapid hydration heat evolution stage begins, the concrete placed in the early morning begins reacting at a higher temperature than concrete placed in the late afternoon, resulting in higher reaction rates, concrete temperatures, and equivalent ages. The effect of the time of placement on equivalent ages is much less dramatic than the effect of air temperatures on equivalent ages.

Vertical profiles of equivalent ages

While the previous results show that the values of t_e averaged over the slab thickness can vary widely depending on ambient conditions and construction variables, concrete temperatures and t_e can also vary with depth within the slab (Fig. 6 and 7). The vertical profiles in Fig. 6 are for points indicated by D, E, and F in Fig. 2(c) and 3(c), and those in Fig. 7 are indicated in Fig. 4(c) and 5(c). In general, the maximum equivalent ages occur near the bottom of the slab, where the maximum concrete temperatures occur, and the minimum equivalent ages occur near the top surface. For the T_a and RH sensitivity simulations, t_e varies by 15 h from bottom to top (Fig. 6(b)). Because up to 85% of the heat transfer occurs at the top surface of the bridge decks (Wojcik and Fitzjarrald 2001), lowest temperatures (Fig. 6(a)) and largest temperature and t_e gradients occur near the top surface.

For the spray water flow rate SW and initial concrete temperature T_{c0} simulations, the top to bottom differences in t_e range from 2 h (D) to 20 h (F) (Fig. 7(b)). For D, with T_{c0} = 5 °C and SW = 0 m^3 h^{-1}, t_e shows almost no vertical variation and concrete temperatures are lower than for E or F (Fig. 7(a)). When the concrete temperatures are lower, the hydration heat generation rates are lower. These low rates allow the boundary forcings (evaporation, convection, runoff water, and net radiation) and diffusion to vertically redistribute heat rapidly compared with the heat production. As a result, the concrete temperatures and resulting values of t_e are more uniform throughout the depth than when the concrete temperatures are higher. For F with T_{c0} = 40 °C and SW = 14 m^3 h^{-1}, the vertical gradients of temperatures (Fig. 7(a)) and t_e (Fig. 7(b)) are greater as higher hydration rates produce more heat within the slab and the maximum spray water flow rate helps to remove this heat at the top surface.

DISCUSSION

The results from this investigation with the SLABS model clearly show that many factors are involved in controlling Class HP concrete temperatures and maturity. Not only must field engineers decide the times of placement and the curing regimens, they must also pay close attention to the atmospheric conditions that occur to ensure that the structure attains the proper maturity within a desired time period before proceeding to other stages of the construction.

Because other concrete mixtures may have different sensitivities to environmental conditions, the results presented here should be viewed as the first attempt to examine such sensitivities, but they are specific to NYSDOT Class HP concrete. Moreover, while a wide variety of conditions were simulated for this study, they are a subset of what can occur and therefore, care must be taken in extrapolating the results presented herein to other situations. Also, the equivalent age data presented herein have not yet been verified with field or laboratory specimens.

The engineer must consider the effect of depth variations of maturity in a concrete structure because during early ages, small differences in equivalent ages represent large differences in strength (for example, Carino 1984). Such variations become important when attempting to determine a representative maturity of a concrete element by a single point measurement of a maturity index. While some portions of the structure may have

reached the specified strength needed for continuing construction or opening a slab to traffic, other portions may not have reached the proper strength. Recognizing this depth variation may be necessary to maintain construction site and public safety. Because most heat transfer and the lowest temperatures occur near the top surface, sampling with a maturity meter near the top surface generally will indicate the lowest maturity attained by the slab—information that will provide a lower limit to the strength development.

The SLABS model indicates that self-desiccation of Class HP concrete may occur at high air temperatures and relative humidities, especially deep within the slab at early ages. Indeed, self-desiccation can occur deep within the slab, especially with high-performance mixtures that contain pozzolans and have a low *w/cm*. Accounting for this self-desiccation when computing maturity indexes will lower their values, perhaps indicating a lower concrete strength at 24 h after placement than indicated by the hydration fractions. The current maturity method, then, provides misleading or unreliable results for concrete in which self-desiccation occurs. There is a need to determine under what conditions and for what mixture proportions such desiccation may occur so that its effect on concrete maturity may be taken into account.

Some of the important construction variables discussed herein (initial concrete temperature and spray water flow rate and temperature) could be controlled by field personnel, if feasible and if desired, to reach acceptable concrete strengths at specified times. These construction variables, then, could be adjusted to offset any problems that could arise due to adverse atmospheric conditions. For example, the initial concrete temperature of a batch of concrete could be lowered to counter the effects of high ambient air temperatures or low wind speeds on concrete temperatures. A simplified field model, such as SLABS, that accounts for all of these factors in predicting concrete temperatures could be an important tool for estimating the expected concrete maturity and temperatures on a case by case basis. Such a planning tool could aid in developing the best quality concrete and maintaining the safety of the construction site, perhaps preventing future disasters like those that occurred at the Skyline Plaza Apartments in Fairfax County, Va., and the Willow Island cooling tower.

SUMMARY AND CONCLUSIONS

In this paper, the SLABS model has been used to investigate the influence of atmospheric and construction conditions on the temperatures and equivalent ages of a concrete bridge deck at 24 h with the following important findings:

1. As long as there is sufficient water available for hydration, maximum equivalent ages coincide with maximum concrete temperatures. For concrete in which self-desiccation occurs, the maturity method can provide misleading results;

2. As expected, equivalent ages after 24 h of hydration averaged over the entire slab thickness are maximum under conditions of high air temperatures and relative humidities, high initial concrete temperatures, low spray water flow rates, and low wind speeds;

3. Over the ranges of variables considered, equivalent ages can vary from 10 to more than 60 h after 24 h of hydration;

4. Equivalent ages are most sensitive to the initial concrete temperature when the spray water flow rate is low, increasing by 25 h (or doubling) over the range of initial concrete temperatures considered;

5. The variations of equivalent ages with depth can exceed 20 h, with the maximum values generally occurring near the bottom of the slab where the maximum concrete temperatures develop. This amount of variation is equivalent to a 40% decrease in equivalent age from the bottom to the top of the slab; and

6. Variations of equivalent age with depth are reduced by a factor of 10 as the initial concrete temperature and spray water flow rate are reduced.

Please contact the author for information about how to obtain the SLABS source code.

ACKNOWLEDGMENTS

The author gratefully acknowledges the funding support of the NIST/NRC Post-doctoral Research Associateship Program. The author wishes to thank the Inorganic Materials Group of the Materials and Construction Research Division in the Building and Fire Research Laboratory at NIST for its support in making this research possible. He also thanks N. Carino, E. Garboczi, N. Martys, and four anonymous reviewers for their comments and suggestions that greatly improved this manuscript.

REFERENCES

ASTM C 1074-98, 1999, "Standard Practice for Estimating Concrete Strength by the Maturity Method," ASTM International, West Conshohocken, Pa., 8 pp.

Bentz, D. P., and Garboczi, E. J., 1991, "Percolation of Phases in a Three-Dimensional Cement Paste Microstructure Model," *Cement and Concrete Research*, V. 21, pp. 325-344.

Brutsaert, W., 1975, "On a Derivable Formula for Longwave Radiation from Clear Skies," *Water Resources Research*, V. 11, pp. 742-744.

Carino, N. J., 1984, "The Maturity Method: Theory and Application," *Cement, Concrete, Aggregates*, V. 6, No. 2, pp. 61-73.

Carino, N. J., and Tank, R. C., 1992, "Maturity Functions for Concretes Made with Various Cements and Admixtures," *ACI Materials Journal*, V. 89, No. 2, Mar.-Apr., pp. 188-196.

Carino, N. J.; Knab, L. I.; and Clifton, J. R., 1992, "Applicability of the Maturity Method to High-Performance Concrete," NISTIR 4819, National Institute of Standards and Technology, Gaithersburg, Md., 62 pp.

Carino, N. J.; Woodward, K. A.; Leyendecker, E. V.; and Fattal, S. G., 1983, "A Review of the Skyline Plaza Collapse," *Concrete International*, V. 5, No. 7, July, pp. 35-42.

Fogler, H. S., 1992, *Elements of Chemical Reaction Engineering*, 2nd Edition, Prentice-Hall, Inc., Englewood Cliffs, N.J., 838 pp.

Freedman, J. M.; Fitzjarrald, D. R.; Moore, K. E.; and Sakai, R. K., 2001, "Boundary Layer Clouds and Vegetation-Atmosphere Feedbacks," *Journal of Climate*, V. 14, pp. 180-197.

Freiesleben-Hansen, P., and Pedersen, J., 1977, "Maturity Computer for Controlled Curing and Hardening of Concrete," *Nordisk Betong*, V. 1, pp. 19-34. (in Danish)

Garboczi, E. J., and Bentz, D. P., 2001, "The Effects of Statistical Fluctuation, Finite Size Error, and Digital Resolution on the Phase Percolation and Transport Properties of the NIST Cement Hydration Model," *Cement and Concrete Research*, V. 31, No. 10, pp. 1501-1514.

Hooton, R. D., 1993, "Influence of Silica Replacement of Cement on Physical Properties and Resistance to Sulfate Attack, Freezing and Thawing, and Alkali-Silica Reactivity," *ACI Materials Journal*, V. 90, No. 2, Mar.-Apr., pp. 143-151.

Incropera, F. P., and DeWitt, D. P., 1996, *Introduction to Heat Transfer*, 3rd Edition, John Wiley & Sons, New York, 801 pp.

Kada-Benameur, H.; Antczak, E.; Broda, M.; and Duthoit, B., 1999, "Contribution to Fluxmeter Measurements to Concrete Maturity Methods," *Materials and Structures*, V. 32, pp. 282-289.

Lew, H. S., 1980, "West Virginia Cooling Tower Collapse Caused by Premature Form Removal," *Journal of Civil Engineering*, ASCE, V. 50, No. 2, pp. 62-67.

Neville, A. M., 1996, *Properties of Concrete*, 4th Edition, Wiley & Sons, New York, 844 pp.

NYSDOT, 1999, "Specification Revisions—Class HP Concrete for Substructures and Structural Slabs," NYSDOT Rep. EI 99-002, New York State Department of Transportation Structures Division, Albany, N.Y., 22 pp.

Pommersheim, J. M., and Clifton, J. R., 1991, "Models of Transport Processes in Concrete," NISTIR 4405, National Institute of Standards and Technology, Gaithersburg, Md., 92 pp.

Powers, T. C., 1958, "Structure and Physical Properties of Hardened Portland Cement Paste," *Journal of the American Ceramic Society*, V. 41, pp. 1-6.

Powers, T. C., and Brownyard, T. L., 1946a, "Studies of Physical Properties of Hardened Portland Cement Paste—Part 1," ACI JOURNAL, *Proceedings* V. 43, Oct., pp. 101-132.

Powers, T. C., and Brownyard, T. L., 1946b, "Studies of Physical Properties of Hardened Portland Cement Paste—Part 1," ACI JOURNAL, *Proceedings* V. 43, Nov., pp. 249-336.

Powers, T. C., and Brownyard, T. L., 1946c, "Studies of Physical Properties of Hardened Portland Cement Paste—Part 3," ACI JOURNAL, *Proceedings* V. 43, Dec., pp. 469-504.

Powers, T. C., and Brownyard, T. L., 1947a, "Studies of Physical Properties of Hardened Portland Cement Paste—Part 4," ACI JOURNAL, *Proceedings* V. 43, Jan., pp. 549-602.

Powers, T. C., and Brownyard, T. L., 1947b, "Studies of Physical Properties of Hardened Portland Cement Paste—Part 5," ACI JOURNAL, *Proceedings* V. 43, Feb., pp. 669-712.

Powers, T. C., and Brownyard, T. L., 1947c, "Studies of Physical Properties of Hardened Portland Cement Paste—Parts 6 and 7," ACI JOURNAL, *Proceedings* V. 43, Mar., pp. 845-880.

Powers, T. C., and Brownyard, T. L., 1947d, "Studies of Physical Properties of Hardened Portland Cement Paste—Parts 8 and 9," ACI JOURNAL, *Proceedings* V. 43, Apr., pp. 933-992.

Prata, A. J., 1996, "A New Long-Wave Formula for Estimating Downward Clear-Sky Radiation at the Surface," *Quarterly Journal of the Royal Meteorological Society*, V. 122, pp. 1127-1151.

Press, W. H.; Teukolsky, S. A.; Vetterling, W. T.; and Flannery, B. P., 1989, *Numerical Recipes in FORTRAN: The Art of Scientific Computing*, Cambridge University Press, New York, 702 pp.

Price, W. H., 1951, "Factors Influencing Concrete Strength," ACI JOURNAL, *Proceedings* V. 47, Feb., pp. 417-432.

Pruppacher, H. R., and Klett, J. D., 1997, *Microphysics of Clouds and Precipitation*, Kluwer Academic Publishers, Dordrecht, The Netherlands, 954 pp.

Stull, R. B., 1988, *An Introduction to Boundary Layer Meteorology*, Kluwer Academic Publishers, Dordrecht, The Netherlands, 666 pp.

Wojcik, G. S., 2001, "The Interaction between the Atmosphere and Curing Concrete Bridge Decks," PhD dissertation, University at Albany, State University of New York, Albany, N.Y., 328 pp.

Wojcik, G. S., and Fitzjarrald, D. R., 2001, "Energy Balances of Curing Concrete Bridge Decks," *Journal of Applied Meteorology*, V. 40, No. 11, pp. 2003-2025.

Wojcik, G. S.; Fitzjarrald, D. R.; and Plawsky, J. L., 2003, "Modeling the Interaction Between the Atmosphere and Curing Concrete Bridge Decks with the SLABS Model," *Meteorological Applications*, V. 10, No. 2, pp. 165-186.

Wojcik, G. S.; Plawsky, J. L.; and Fitzjarrald, D. R., 2001, "Development of a Bimolecular Expression to Describe the Heat Generation of Class HP Concrete," *Cement and Concrete Research*, V. 31, No. 12, pp. 1847-1858.